

Supporting Information

Electronic Structure of the Plasmons in Metal Nanocrystals: Fundamental Limitations for the Energy Efficiency of Hot Electron Generation

Le Chang^{1,a}, Lucas V. Besteiro^{1,2,a*}, Jiachen Sun¹, Eva Yazmin Santiago⁴, Stephen K. Gray³,
Zhiming Wang^{1*}, Alexander O. Govorov^{1,4*}

¹ *Institute of Fundamental and Frontier Sciences, University of Electronic Science and Technology of China, Chengdu 610054, China*

² *Centre Énergie Matériaux et Télécommunications, Institut National de la Recherche Scientifique, Varennes, Québec J3X 1S2, Canada*

³ *Center for Nanoscale Materials, Argonne National Laboratory, Lemont, IL 60439, USA*

⁴ *Department of Physics and Astronomy, Ohio University, Athens OH 45701, USA*

* Corresponding authors: lucas.besteiro@emt.inrs.ca; zhmwang@uestc.edu.cn;
govorov@ohio.edu

^a Author Contributions: L.C. and L.V.B. contributed equally.

1. Boltzmann formalism for the 3D case

We now start from the Boltzmann equation (see the textbook [S1]):

$$\frac{\partial f_{\mathbf{k}}}{\partial t} + \mathbf{v}_{\mathbf{k}} \cdot \nabla_{\mathbf{r}} f_{\mathbf{k}} + \frac{e\mathbf{E}}{\hbar} \cdot \nabla_{\mathbf{k}} f_{\mathbf{k}} = -\frac{f_{\mathbf{k}} - f_{\mathbf{F}}^0}{\tau_{\text{rel}}}, \quad (\text{S1})$$

where the external field $\mathbf{E} = \text{Re}[\mathbf{E}_{\omega} \cdot e^{-i\omega t + i\mathbf{q}\mathbf{r}}]$; here \mathbf{q} is the wavevector of the external perturbation acting on the Fermi gas. The Fermi distribution function at equilibrium is

$$f_{\mathbf{F}}^0(E_{\mathbf{k}}, T_e) = \frac{1}{e^{\frac{E_{\mathbf{k}} - E_{\mathbf{F}}}{k_{\text{B}} T_e}} + 1}.$$

First, for simplicity, we neglect the second term in (S1) assuming the long-wavelength limit, $\omega \gg q \cdot v_{\text{F}}$, where $q = 2\pi / \lambda$ and λ is the wavelength of the perturbation in the electron gas. In other words, we look at the limit $q \rightarrow 0$. Then, we have

$$\frac{\partial f_{\mathbf{k}}}{\partial t} + \frac{e\mathbf{E}}{\hbar} \cdot \nabla_{\mathbf{k}} f_{\mathbf{k}} = -\frac{f_{\mathbf{k}} - f_{\mathbf{F}}^0}{\tau_{\text{rel}}} \quad (\text{S2})$$

Within the perturbation theory, we seek a solution in the form:

$$f_{\mathbf{k}} = f_{\mathbf{F}}^0 + f_1 + f_2 + \dots \quad (\text{S3})$$

where $f_n \propto E_{\omega}^n$. The first term is typically derived in textbooks [S1] as it gives the linear response and the related electric conductivity of an electron gas:

$$f_1 = \text{Re}[\delta f_1 e^{-i\omega t}]. \quad (\text{S4})$$

Linearization of (S2) yields

$$-i\omega\delta f_1 + \frac{e\mathbf{E}}{\hbar} \cdot \nabla_{\mathbf{k}} f_F^0 = -\frac{\delta f_1}{\tau_{\text{rel}}}.$$

Then, since $\nabla_{\mathbf{k}} f_F^0 = \hbar \mathbf{v}_{\mathbf{k}} \frac{\partial f_F^0}{\partial E_{\mathbf{k}}}$, we obtain

$$\delta f_1 = -\frac{e\tau_{\text{rel}}(\mathbf{v}_{\mathbf{k}} \cdot \mathbf{E}_{\omega})}{1 - i\omega\tau_{\text{rel}}} \frac{\partial f_F^0}{\partial E_{\mathbf{k}}}. \quad (\text{S5})$$

The above function yields the leading contribution in (S4). The term $f_1 = \text{Re}[\delta f_1 e^{-i\omega t}]$ oscillates in time and describes the electric current in the system. The steady-state contribution to the nonequilibrium distribution function (which is not oscillating) should be found as the function $\langle f_2 \rangle_{\text{time}}$. For this, we will now collect the nonlinear, quadratic terms from (S3) into (S2):

$$\frac{\partial f_2}{\partial t} + \frac{e\mathbf{E}}{\hbar} \cdot \nabla_{\mathbf{k}} f_1 = -\frac{f_2}{\tau_{\text{rel}}}$$

Since we are interested in the time-independent term (steady-state distribution under excitation), we perform time-averaging the above equation:

$$\left\langle \frac{e\mathbf{E}}{\hbar} \cdot \nabla_{\mathbf{k}} f_1 \right\rangle = -\frac{\langle f_2 \rangle}{\tau_{\text{rel}}}$$

That gives us the expression

$$\langle f_2 \rangle = -\tau_{\text{rel}} \frac{1}{2} \frac{e}{\hbar} \text{Re}[\mathbf{E}_{\omega} \cdot \nabla_{\mathbf{k}} f_1^*]$$

Then, by using (S5), we obtain:

$$\langle f_2 \rangle = \tau_{\text{rel}} A(\omega, E_{\mathbf{k}}) \frac{\partial^2 f_{\text{F}}^0}{\partial E_{\mathbf{k}}^2}. \quad (\text{S6})$$

The above function is shown in the main text as Eq. 12. Its main property is its energy dependence through $\frac{\partial^2 f_{\text{F}}^0}{\partial E_{\mathbf{k}}^2}$. We show it below in Fig. S1, where we observe that the excited electrons and holes are found near the Fermi level, within the thermal interval $6k_{\text{B}}T$. Coming back to (S6), the physical meaning of the function $A(\omega, E)$ can be retrieved from the following consideration: The term $-\frac{f_2}{\tau_{\text{rel}}}$ produces the local dissipation in our system,

$$q_{\text{dissipation}}(\omega) = \int_0^{\infty} E \cdot \frac{f_2}{\tau_{\text{rel}}} \text{DOS}(E) dE = \langle \mathbf{j} \cdot \mathbf{E} \rangle_{\text{time}},$$

where $\text{DOS}(E)$ is the density of electronic states. Therefore,

$$\begin{aligned} q_{\text{dissipation}}(\omega) &= \int_0^{\infty} E \cdot A(\omega, E) \frac{\partial^2 f_{\text{F}}^0}{\partial E_{\mathbf{k}}^2} \text{DOS}(E) dE \\ &\approx - \int_0^{\infty} E \cdot A(\omega, E) \cdot \delta'(E - E_{\text{F}}) \cdot \text{DOS}(E) dE \\ &= [E \cdot A(\omega, E) \cdot \text{DOS}(E)]'_{E=E_{\text{F}}} \end{aligned}$$

Above, we used the following property of the Fermi function at low temperature:

$$\frac{\partial^2 f_{\text{F}}^0}{\partial E_{\mathbf{k}}^2} \approx -\delta'(E_{\mathbf{k}} - E_{\text{F}})$$

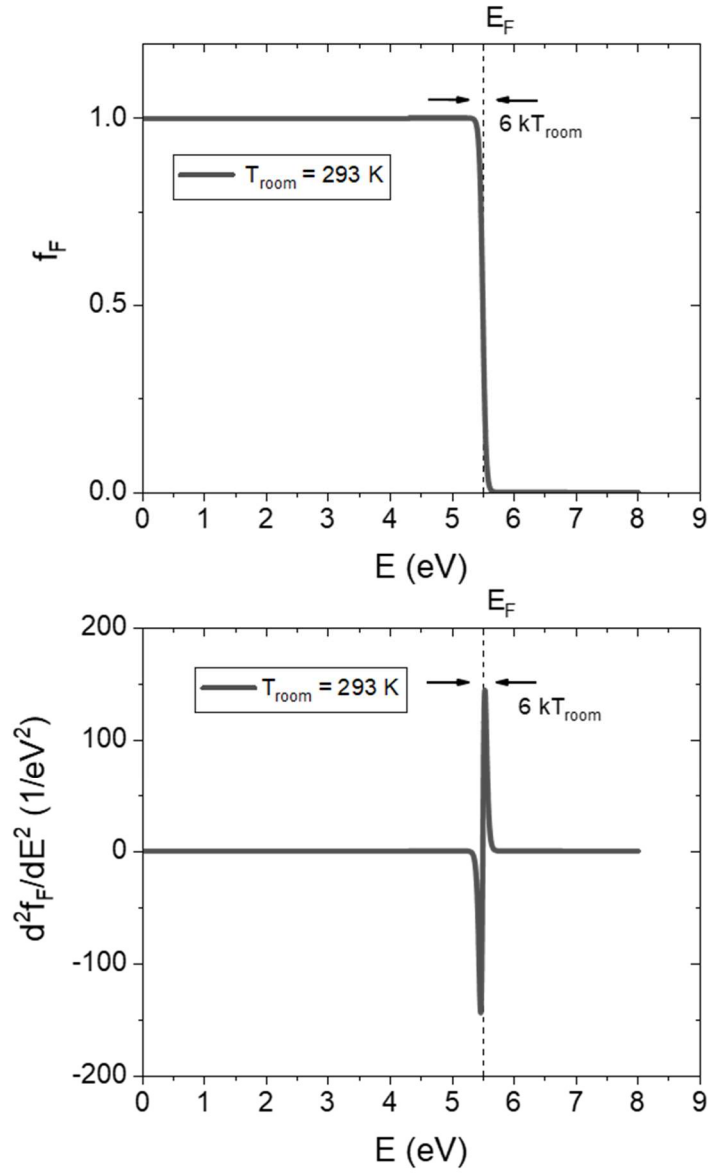


Figure S1: The Fermi distribution and its second derivative in gold at room temperature. Here T_{room} denotes the room temperature (293K or 20°C). The second derivative of the Fermi function provides us with the energy distribution of excited carriers in the electron gas when driven by an external field. We observe that, within the linear quasi-classical theory, all electronic events occur in the very vicinity of the Fermi level. The physical reason is that the Fermi energy in a noble metal is typically very large, so that $E_F \gg k_B T_{room}$ or $T_F \gg T_{room}$, where $T_F = E_F / k_B$ is the Fermi temperature. For gold and silver, $E_F \sim 5.5$ eV that yields the Fermi temperature of $T_F \sim 64000$ K.

2. The number of photogenerated plasmons and the phototemperature.

We now consider how many plasmons are stored in an optically-driven NC. The rate equation for the number of plasmons reads [S2]:

$$\frac{dN_{\text{plasmons}}}{dt} = \frac{Q_{\text{abs}}}{\hbar\omega_p} - \frac{N_{\text{plasmons}}}{\tau_{\text{plasmon}}} \quad (\text{S7})$$

where N_{plasmons} is the number of plasmons stored in a NC, $\hbar\omega_p$ is the plasmon quantum and Q_{abs} is the energy absorption rate at the plasmon peak. The term $\frac{Q_{\text{abs}}}{\hbar\omega_p}$ in (S7) is the rate of creation of plasmons by light.

Figure S2a depicts a theoretical model for the nonlinear regime of excitation, in which a few plasmons can be excited in a single NC. Below we will see that, under CW illumination, it is challenging to achieve a situation with a few excited plasmons in a single NC. However, as we mentioned in the main text, the regime with a few pumped plasmons in a single NC can be achieved under excitation with powerful ultrashort pulses, [S3] when the lattice temperature may not increase so significantly.

In the CW regime, the time derivative in (S7) vanishes and we obtain a simple estimate for the plasmonic population

$$N_{\text{plasmons}} = \frac{Q_{\text{abs}}}{\hbar\omega_p} \tau_{\text{plasmon}} \quad (\text{S8})$$

Assuming a plasmon to be a simple harmonic oscillator, the relaxation rate for the population of plasmon is $1/\tau_{\text{plasmon}} = 2\gamma_{\text{plasmon,dec}}$, where $\gamma_{\text{plasmon,dec}}$ is the decoherence rate. This decoherence rate should be taken as half of the broadening of the plasmon peak in the absorption spectrum, since such broadening comes from the decoherence of oscillations of the polarization. In other words, $\gamma_{\text{plasmon,dec}} = FWHM/2$ for the plasmonic peak. For a spherical NC, we can see from simple simulations within the local dielectric function approach that $\tau_{\text{plasmon}} = 2.4$ fs. This time is shorter

than the time constant coming directly from the Drude relaxation constant: $\gamma_{\text{Drude}} = 0.078 \text{ eV}$ and $\tau_{\text{Drude}} = \hbar / (\gamma_{\text{Drude}}) = 8.4 \text{ fs}$. The reason is that the plasmon peak in a spherical NC is strongly broadened due to the interband transitions. The absorption rate is calculated from the Mie theory using the standard equation:

$$Q_{\text{abs}} = \sigma_{\text{abs}} \cdot I_0,$$

$$\sigma_{\text{abs}} = \frac{\omega}{c\sqrt{\epsilon_{\text{matrix}}}} \frac{4\pi R_0^3}{3} \left| \frac{3\epsilon_{\text{matrix}}}{2\epsilon_{\text{matrix}} + \epsilon_{\text{metal}}} \right|^2 \text{Im}[\epsilon_{\text{metal}}],$$

where ϵ_{metal} is taken from the tables [S4] and the light flux I_0 is a variable. We need to consider two models: a NC in water (model 1) and a NC on a glass substrate (model 2). Figures S2 and S3 below show such models. For those models, we take the following dielectric constants for the matrix: $\epsilon_{\text{matrix}} = 1.8$ (water) and $\epsilon_{\text{matrix}} = (1 + 2.5) / 2 = 1.75$ (a NC on a substrate).

Simultaneously, we should estimate the photoinduced temperature by a NC. For a spherical NC, we have for the local increase of temperature at the surface:

$$\Delta T_{\text{NC,surface}} = \frac{q_{\text{NC}}}{4\pi k_{\text{t,matrix}} R_{\text{NC}}}, \quad (\text{S9})$$

where R_{NC} is the NC radius and $k_{\text{t,matrix}}$ is the heat conductivity. For the first model, $k_{\text{t,matrix}} = k_{\text{t,water}} = 0.6 \text{ W}/(\text{cm} \cdot \text{K})$. In the second case, we can take the thermal conductivity as an average of glass and air: $k_{\text{t,matrix}} = (k_{\text{t,glass}} + k_{\text{t,air}}) / 2 \approx 0.7 \text{ W}/(\text{cm} \cdot \text{K})$.

Below we present the results for a 40 nm Au NC under CW pumping for both models. We excite the NC exactly at the plasmon peak, i.e. at $\omega = \omega_{\text{p}}^{\text{NC}}$, where $\hbar\omega_{\text{p}}^{\text{NC}} = 2.37 \text{ eV}$; the corresponding wavelength of excitation is $\lambda_{\text{p}}^{\text{NC}} = 520 \text{ nm}$.

2.1 Model 1: Water matrix

Local heating regime: Figure S2a shows the number of plasmons and the photoinduced local temperature. The local temperature at the surface was calculated as

$$T_{NP,surface} = \Delta T_{NP,surface} + 293 \text{ K} .$$

The room temperature was taken as 20 °C, thus in absolute units is 293K. Then, the boiling point for water will be reached when the phototemperature of $\Delta T_{NP,surface} = 80 \text{ K}$. We reach such temperature for $I_0 = 3.6 \cdot 10^5 \text{ W/cm}^2$. For that intensity, the number of plasmons is $N_{plasmons} \approx 0.08 \ll 1$. Therefore, for the case of water matrix, the steady-state number of plasmon at the boiling point of the matrix is small. In other words, we may not be able to achieve a large population of plasmons in a liquid matrix under the CW illumination regime.

Collective heating regime: We should also emphasize that the above temperature (S9) is the local one. In real experiments with NC solutions, the temperature is typically given by the collective heating effect [S5,S6], which produces temperatures much greater than the above estimate, $\Delta T_{NC,surface}$, given by (S9). In the model shown in Figure S2c, we observe that $\Delta T_{collective} \gg \Delta T_{NC,surface}$. Now we will compute the collective temperature at the center of a spherical cluster composed of 10^5 NCs. The cluster is submerged in a boundless water matrix. The equations to compute the collective temperature are [S5]:

$$\Delta T_{collective} = \frac{3}{2} \frac{Q_{tot}}{4\pi k_{t,matrix} R_0} \frac{1}{R_0} = \frac{3}{2} \frac{q_{NC}}{4\pi k_{t,matrix} R_{NC}} \cdot N_{NC} \frac{R_{NC}}{R_0} = \frac{3}{2} \Delta T_{NC,surface} \cdot N_{NC} \frac{R_{NC}}{R_0}$$

$$Q_{tot} = q_{NC} \cdot N_{NC}$$

where Q_{tot} is the total absorption rate, N_{NC} is the number of Au NCs in the cluster, R_0 is the radius of the cluster. The parameters used in the calculations are: $N_{NC} = 10^5$ and $R_0 = 5.8 \text{ } \mu\text{m}$.

The calculated collective temperature is, of course, much higher than the local one. The collective enhancement factor is

$$Enh_{collective} = \frac{\Delta T_{collective}}{\Delta T_{NP,surface}} \approx 521.$$

Figure S2c shows the collective phototemperature. The boiling point is now reached at the smaller intensity of $I_0 = 0.68 \cdot 10^3 \text{ W/cm}^2$. Then, the plasmon number per a NC is now really small at the boiling point: $N_{\text{plasmons}} \approx 0.00015 \ll 1$. Again, we observe that the number of plasmons per NC is small for the typical intensities used in a solution experiment.

2.2 Model 2: A NC on a substrate

In model 2, we look at the local heating effect arising from a single NC placed on a glass surface (Figure S3). Again, we estimate the number of plasmons and the corresponding phototemperature. In this system, the relevant phase transition is the melting of the gold NC. Bulk gold melts at 1337 K (1064 °C), although a small NC can reshape or melt at lower temperatures [S7]. We again observe an interesting picture - the pumping of a single plasmon in the CW regime is challenging. The required flux for the condition $N_{\text{plasmons}} = 1$ is $I_0 = 4.9 \cdot 10^6 \text{ W/cm}^2$. Simultaneously, the flux required to melt the NC is very close to the above number, with $I_{0,\text{melting}} = 5.8 \cdot 10^6 \text{ W/cm}^2$. Therefore, we observe an interesting property: maintaining a single plasmon into a NC in the steady state comes together with melting the NC. In a real experiment, it can be challenging to achieve a regime with $N_{\text{plasmons}} \sim 1$ in a single NC, because the NC can be damaged at the required excitation intensity.

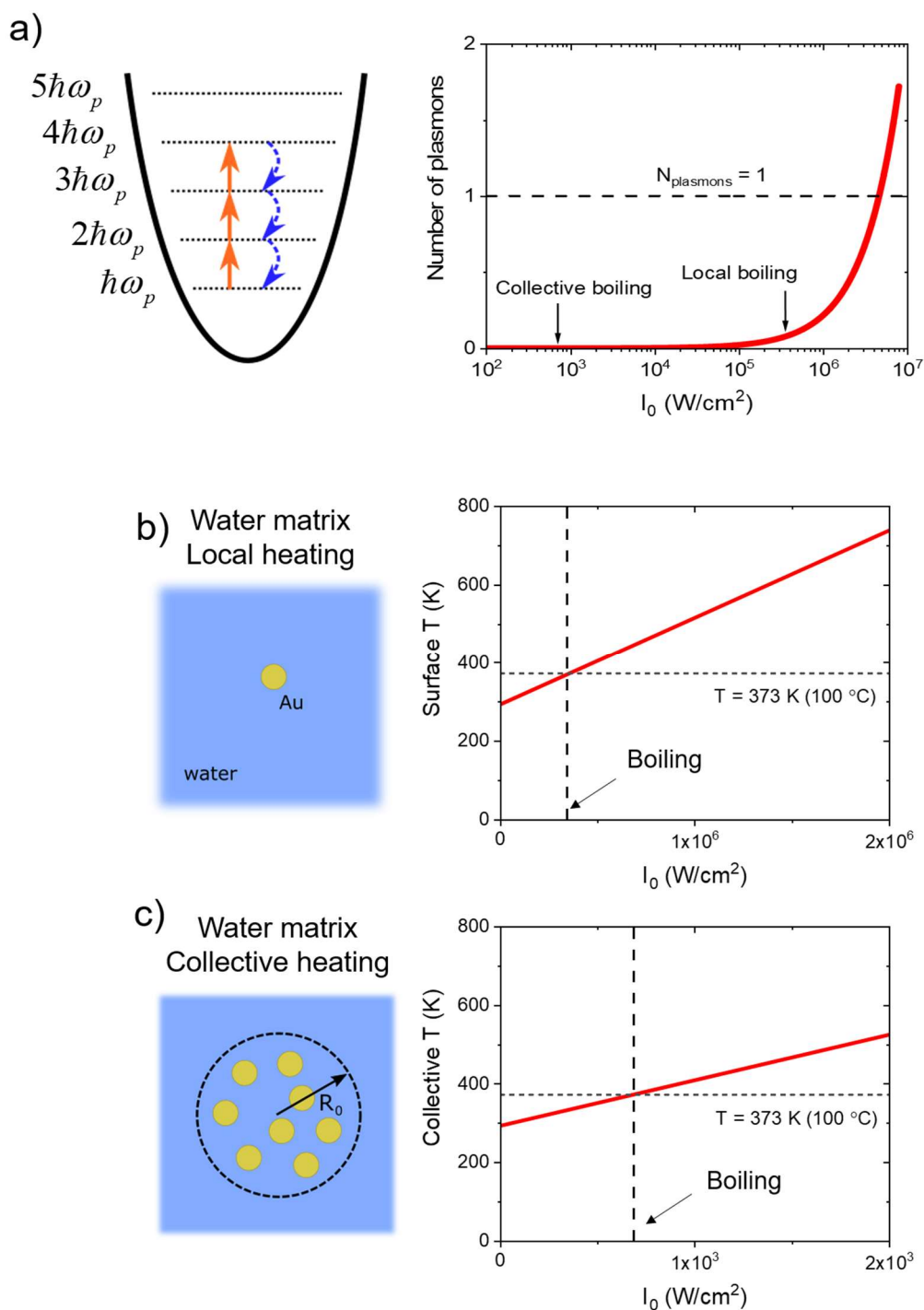


Figure S2: **a)** Energy diagram for the nonlinear regime of multi-plasmon generation and the calculated number of plasmons in one NC in the CW excitation regime. **b,c)** Phototemperature. The phototemperature is calculated for the two cases. Panel (b) shows the regime of local heating using a single spherical NC. Panel (c) describes the case with the strong collective heating effect; in this case we use the model of a cluster of Au NCs.

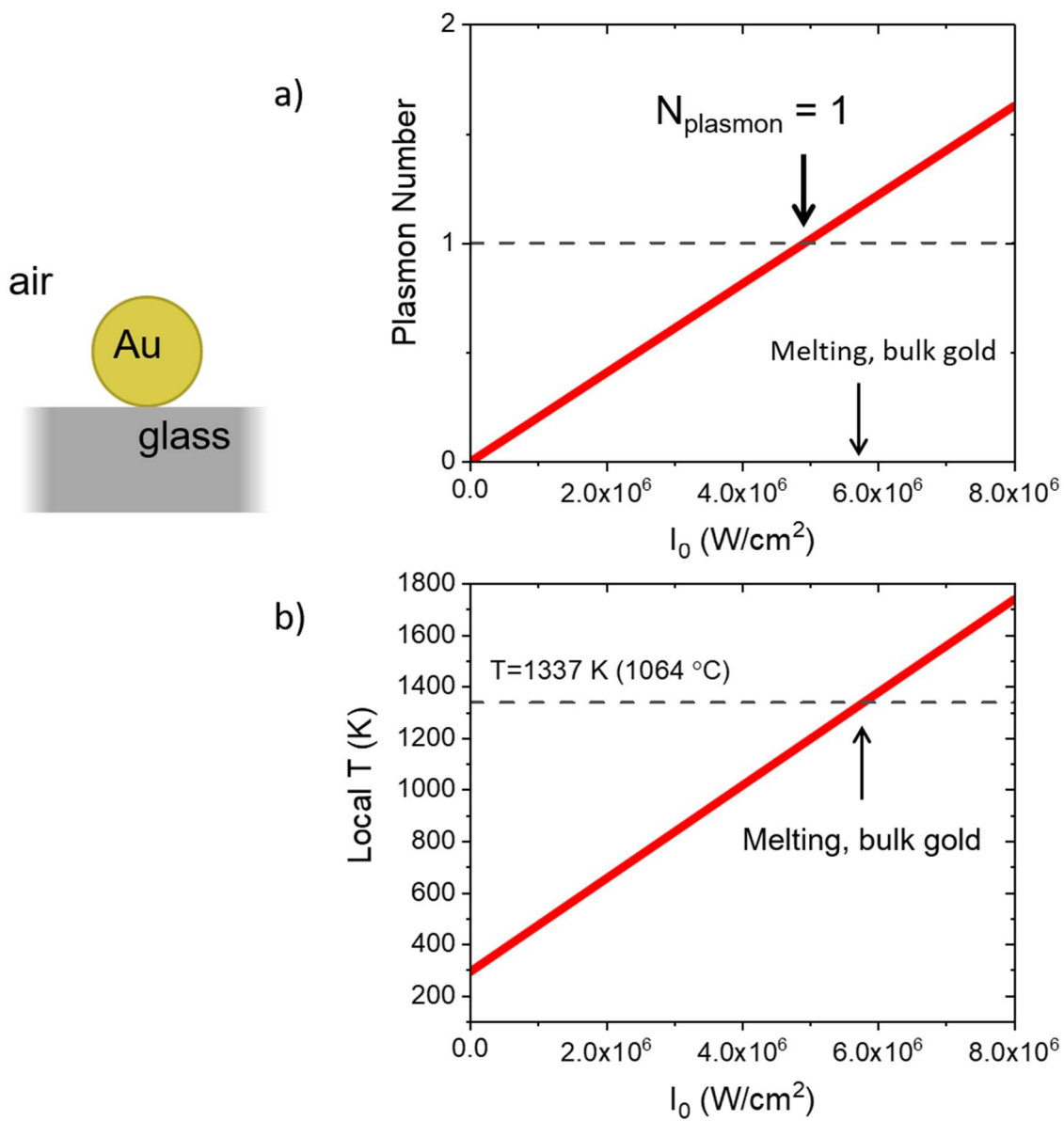


Figure S3: a) Number of plasmons in a single NC phototemperature in the model incorporating a single NC on a glass substrate (diagram on the left). **b)** Local temperature at the NC. The relevant phase transformation in this case is the melting of the gold NC.

3. Current literature on HEs.

Here we give a few examples of fully-quantum calculations for the energy distribution of HEs in a plasmonic NCs. The authors of the data shown in Figure S4 employed different theoretical approaches. In these spectra, one can see two types of excited carriers: the HEs with high energies and the plasmonic (Drude) electrons with low excitation energies. The HEs are created via quantum optical transitions in a NC. The plasmonic low-energy carriers occupy the states near the Fermi level and appear as a result of classical acceleration.

Steady State HE distributions from the current literature

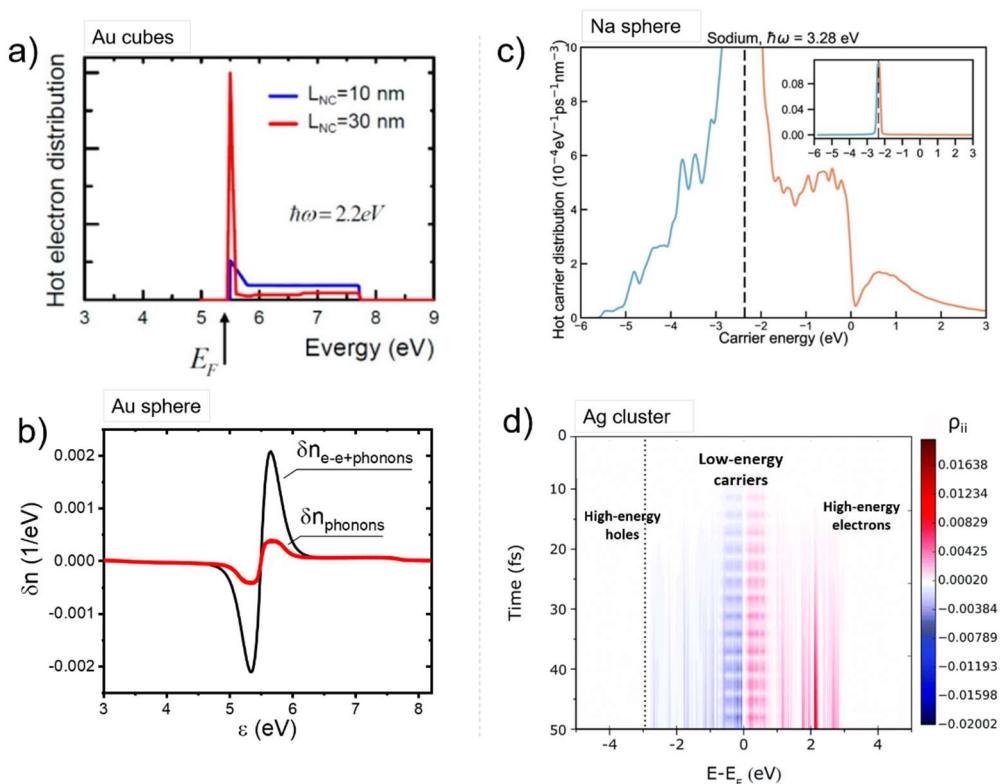


Figure S4: A few examples of calculated hot-electron distributions from the current literature. These distributions were calculated for various nanocrystals, which were optically driven at the plasmonic frequency. **a)** Au cubes from [S2]. The approach is based on the density matrix formalism. **b)** Au spheres from [S8]. The approach is based on the density matrix formalism and the mean-field theory. **c)** Sodium sphere from [S9]. The method involves Fermi's golden rule. **d)** TD-DFT calculation for the large Ag cluster from [S10]. Reproduced with permission from (a) [S2] Copyright 2013 American Chemical Society, (b) [S8] Copyright 2017 American Chemical

4. Estimates for nonthermalized hot electrons and for thermalized hot carriers.

Figure 7a shows that an excited NC always has some number of nonthermalized HEs with energies in the interval $E_F < E < E_F + \hbar\omega$. Then, Figures 10a,b give another piece of information: for certain experimental situations, we specifically care about the numbers of over-barriers electrons, i.e. the number of electrons with $E > \Delta E_{\text{bar}}$. There are two mechanisms creating such carriers: the direct optical excitation and the electronic photothermal effect. We now estimate the number of over-barrier carriers for those mechanisms.

First, we define the electronic temperature as a function of the intensity for a typical experimental situation. We note that the electronic and crystal temperatures are close to each other in the CW excitation regime. From the experiment [S11], we derive the following function:

$$\begin{aligned} T_e &= T_{\text{room}} + \Delta T = T_{\text{room}} + \alpha_T I_0 \\ T_{\text{room}} &= 293 \text{ K } (20 \text{ }^\circ\text{C}) \end{aligned}, \quad (\text{S10})$$

where the photothermal coefficient is calculated as

$$\alpha_T = \frac{80 \text{ K}}{566 \text{ W/cm}^2}.$$

This coefficient is derived from the observation that the solution gets boiled at the flux of 566 W/cm^2 . The mechanism of photo-heating is collective and, therefore, we need relatively small intensities to reach the boiling point of water. The Au spherical NCs in Ref. [S11] had a diameter of 40nm. The optical path and the laser spot radius were 1.65 mm and 0.15 mm, respectively. The NC concentration was $9 \cdot 10^{10} \text{ cm}^{-3}$. Now we compute the number of thermal electrons in a NC above the barrier. For high energies ($E - E_F \gg k_B T_e$), the Fermi distribution function becomes an exponential function:

$$f_F^0(E, T_e) = \frac{1}{\frac{E-E_F}{k_B T_e} + 1} \approx e^{-\frac{E-E_F}{k_B T_e}}$$

$$T_e = T_e(I_0)$$

Then, the number of over-barriers electrons is computed in the following way:

$$N_{\text{Thermal HE, } E > \Delta E_{\text{bar}}}(I_0) = \int_{E_F + \Delta E_{\text{bar}}}^{\infty} \text{DOS}(E) f_F^0(E, T_e) dE$$

$$\approx \text{DOS}(E_F + \Delta E_{\text{bar}}) \int_{E_F + \Delta E_{\text{bar}}}^{\infty} e^{-\frac{E-E_F}{k_B T_e}} dE \quad (\text{S11})$$

$$= \text{DOS}(E_F + \Delta E_{\text{bar}}) \cdot k_B T_e e^{-\frac{\Delta E_{\text{bar}}}{k_B T_e}} \propto e^{-\frac{\Delta E_{\text{bar}}}{k_B T_e}}$$

where $\text{DOS}(\varepsilon)$ is the density of states in a NC:

$$\text{DOS}_e(\varepsilon) = V_{\text{NC}} \frac{m}{\pi^2 \hbar^3} \sqrt{2m\varepsilon}$$

Here V_{NC} is the NC volume. Eq. (S11) is the key formula to estimate the number of photothermal electrons in a NC. It has the Boltzmann exponential function, which is very small at small light intensities, since $\Delta E_{\text{bar}} \gg k_B T_e$. Here T_e is the electronic temperature and this temperature $T_e \sim T_{\text{room}}$. To get the feeling of how small this function is, we now look at the involved energies and their ratio: $\Delta E_{\text{bar}} = 0.8 \text{ eV}$, $k_B T_{\text{room}} = 0.025 \text{ eV}$ and $\Delta E_{\text{bar}} / k_B T_{\text{room}} \sim 31.7$. Therefore, the exponential function at room temperature becomes

$$e^{-\frac{\Delta E_{\text{bar}}}{k_B T_{\text{room}}}} \approx 1.7 \times 10^{-14}$$

However, the coefficient before the exponential function in (S11) is large. So, we need to be careful in computing function (S11). To quantify the electronic photothermal process, we will plot below the photo-induced change in the thermal over-barrier population:

$$\delta N_{\text{Thermal HE, } E > \Delta E_{\text{bar}}} (I_0) = N_{\text{Thermal HE, } E > \Delta E_{\text{bar}}} (I_0) - N_{\text{Thermal HE, } E > \Delta E_{\text{bar}}} (0) \quad (0)$$

The number of HE electrons can be derived from the rate of generation and the relaxation time. Under the steady-state condition, the number of HEs is given by

$$\delta N_{\text{HE, } E > \Delta E_{\text{bar}}} = \text{Rate}_{\text{HE, } E > \Delta E_{\text{bar}}} \cdot \bar{\tau}_{\text{e-e}} \quad (\text{S12})$$

where $\text{Rate}_{\text{HE, } E > E_F + \Delta E_{\text{bar}}}$ is the rate of generation of HEs and $\bar{\tau}_{\text{e-e}}$ is the e-e relaxation time. The rate of the HE production is given in the main text as Eq. 19:

$$\text{Rate}_{\text{HE, } E > E_F + \Delta E_{\text{bar}}} = \frac{1}{4} \frac{2}{\pi^2} \frac{e^2 E_F^2}{\hbar} \frac{\hbar\omega - \Delta E_{\text{bar}}}{(\hbar\omega)^4} \int_S |E_{\omega, \text{normal}}|^2 ds \quad (\text{S13})$$

The e-e relaxation time as a function of energy is given by:

$$\tau_{\text{e-e}}(\mathcal{E}) = \tau_{0, \text{e-e}} \frac{E_F^2}{(\mathcal{E} - E_F)^2}$$

where $\tau_{0, \text{e-e}} = 6$ fs [S12]. For our numerical estimates, we will take the e-e time in the middle of the energy interval of interest, which is $E_F + \Delta E_{\text{bar}} < E < E_F + \hbar\omega$, where $\hbar\omega = 2.37$ eV and $\Delta E_{\text{bar}} = 0.8$ eV. In other words, we take $\bar{\tau}_{\text{e-e}} = \tau_{\text{e-e}}(\bar{\mathcal{E}})$, where $\bar{\mathcal{E}} = 1.59$ eV.

For a spherical NC, the surface integral in (S13) is easy to compute [S13]:

$$\text{Rate}_{\text{HE, } E > E_F + \Delta E_{\text{bar}}} = \frac{1}{4} \frac{2}{\pi^2} \times \frac{e^2 E_F^2}{\hbar} \frac{(\hbar\omega - \Delta E_b)}{(\hbar\omega)^4} \frac{4\pi}{3} R_0^2 \left| \frac{3\epsilon_{\text{water}}}{2\epsilon_{\text{water}} + \epsilon_{\text{metal}}} \right| \tilde{E}_0^2$$

$$I_0 = \frac{c_0 \sqrt{\epsilon_{\text{water}}}}{8\pi} \cdot |\tilde{E}_0|^2$$

where \tilde{E}_0 is the amplitude of the external driving field, which is taken in the standard form $E(t) = \tilde{E}_0 \cos(\omega t)$.

From the key equations (S11) and (S12), we observe that

$$\begin{aligned}\delta N_{\text{Thermal HE, } E > \Delta E_{\text{bar}}} &\propto e^{-\frac{\Delta E_{\text{bar}}}{k_{\text{B}} T_{\text{c}}(I_0)}} \\ \delta N_{\text{HE, } E > \Delta E_{\text{bar}}} &\propto I_0 (\hbar \omega - \Delta E_{\text{bar}})\end{aligned}$$

For the case of the thermalized HEs, we assumed above that $e^{-\frac{\Delta E_{\text{bar}}}{k_{\text{B}} T_{\text{c}}(I_0)}} \gg e^{-\frac{\Delta E_{\text{bar}}}{k_{\text{B}} T_{\text{room}}}}$. The above dependencies are fundamentally different. The number of HEs has a linear dependence with the intensity, whereas the number of thermal HEs is proportional to the exponential function, in which the intensity enters the Boltzmann exponent. Therefore, the HEs will always dominate for small light intensities. Below we will see it this in our numerical calculations (Figure S5). At the intensity required to boil water in a solution system, the number of HEs is much greater than the number of thermal electrons:

$$\begin{aligned}\text{Ratio} &= \frac{\delta N_{\text{HE, } E > \Delta E_{\text{bar}}}}{\delta N_{\text{Thermal HE, } E > \Delta E_{\text{bar}}}} \sim 691 \\ I_0 &= 566 \text{ W/cm}^2\end{aligned}$$

The above estimates for realistic experimental conditions show the importance of HEs in small plasmonic nanostructures, where the quantum surface generation of HEs dominates over the bulk electronic photothermal effect. Figure S5 illustrates this conclusion.

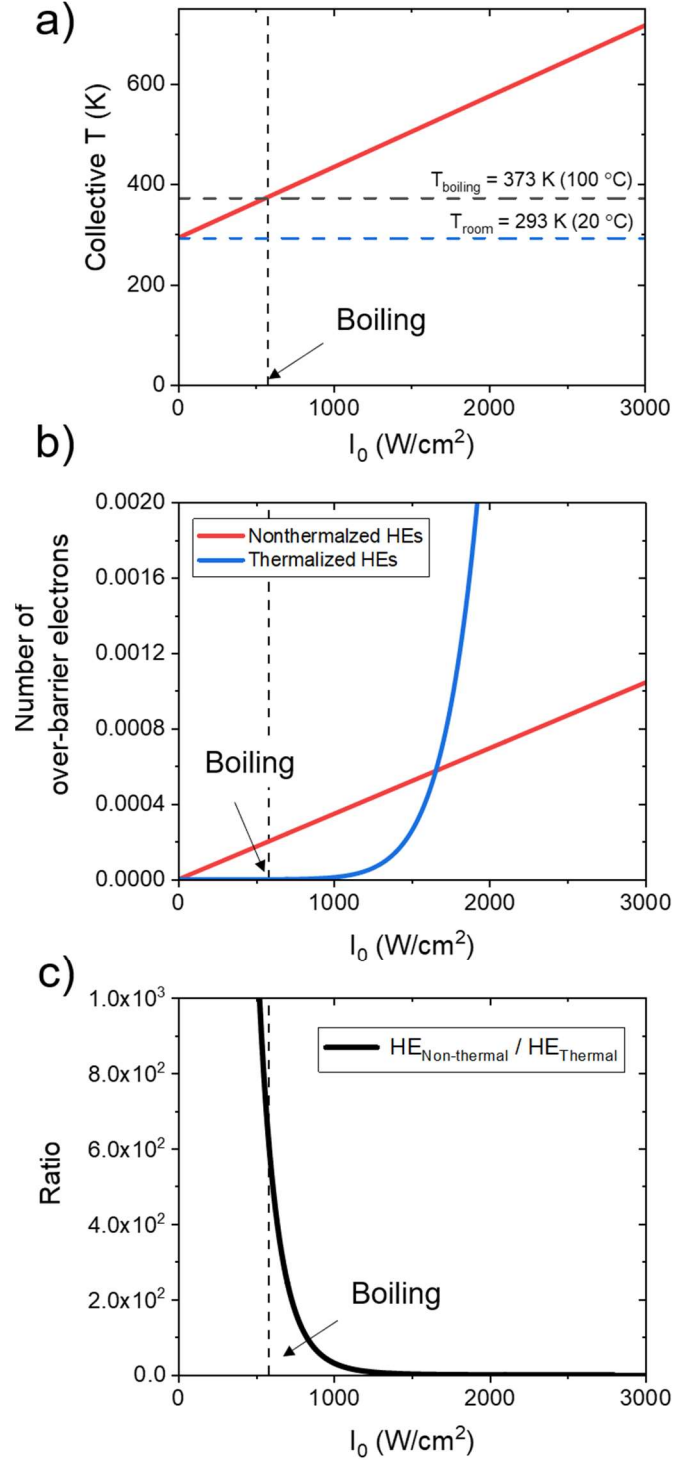


Figure S5: This figure includes the calculated collective phototemperature (a), the numbers of over-barrier electrons (b) and the ratio, $\text{Ratio} = \delta N_{\text{HE, } E > \Delta E_{\text{bar}}} / \delta N_{\text{Thermal HE, } E > \Delta E_{\text{bar}}}$ (c). Here, we used the following parameters: $E_{\text{F}} = 5.5 \text{ eV}$ (gold), $\Delta E_{\text{bar}} = 0.8 \text{ eV}$ (Au-TiO₂ barrier) and $\epsilon_{\text{water}} = 1.8$. Pumping is resonant, i.e. $\hbar\omega = \hbar\omega_{\text{p}}^{\text{NC}} = 2.37 \text{ eV}$ (520 nm).

References:

- [S1] Tanner, D. B. *Optical Effects in Solids*, 1st ed.; Cambridge University Press: Cambridge, U.K., 2019.
- [S2] Govorov, A. O.; Zhang, H.; Gun'ko, Y. K. Theory of Photoinjection of Hot Plasmonic Carriers from Metal Nanostructures into Semiconductors and Surface Molecules. *J. Phys. Chem. C* **2013**, *117* (32), 16616–16631.
- [S3] Besteiro, L. V.; Yu, P.; Wang, Z.; Holleitner, A. W.; Hartland, G. V.; Wiederrecht, G. P.; Govorov, A. O. The Fast and the Furious: Ultrafast Hot Electrons in Plasmonic Metastructures. Size and Structure Matter. *Nano Today* **2019**, *27*, 120–145.
- [S4] Johnson, P. B.; Christy, R. W. Optical Constants of the Noble Metals. *Phys. Rev. B* **1972**, *6*, 4370.
- [S5] Govorov, A.O.; Zhang, W.; Skeini, T.; Richardson, J.; Lee, J.; Kotov, N. Gold Nanoparticle Ensembles as Heaters and Actuators: Melting and Collective Plasmon Resonances. *Nanoscale Res. Lett.* **2006**, *1*, 84–90.
- [S6] Richardson, H. H.; Carlson, M. T.; Tandler, P.J.; Hernandez, P.; Govorov, A. O. Experimental and Theoretical Studies of Light-to-Heat Conversion and Collective Heating Effects in Metal Nanoparticle Solutions, *Nano Lett.* **2009**, *9* (3), 1139-1146.
- [S7] Schmid, G., Corain, B. Nanoparticulated Gold: Syntheses, Structures, Electronics, and Reactivities. *Journal of Inorganic Chemistry.* **2003**, *17*, 3081-3098.
- [S8] Besteiro, L. V.; Kong, X.-T.; Wang, Z.; Hartland, G.; Govorov, A. O. Understanding Hot-Electron Generation and Plasmon Relaxation in Metal Nanocrystals: Quantum and Classical Mechanisms. *ACS Photonics* **2017**, *4* (11), 2759–2781.
- [S9] Dal Forno, S.; Ranno, L.; Lischner, J. Material, Size, and Environment Dependence of Plasmon-Induced Hot Carriers in Metallic Nanoparticles. *J. Phys. Chem. C* **2018**, *122* (15), 8517–8527.
- [S10] Douglas-Gallardo, O. A.; Berdakin, M.; Frauenheim, T.; Sanchez, C. G. Plasmon-Induced Hot-Carrier Generation Differences in Gold and Silver Nanoclusters. *Nanoscale* **2019**, *11*, 8604–8615.
- [S11] Baral, B.; Green, A.; Livshits, M.; Govorov, A.; Richardson, H. H. Comparison of Vapor Formation of Water at the Solid/Water Interface to Colloidal Solutions Using Optically Excited Gold Nanostructures. *ACS Nano* **2014**, *8* (2), 1439-1448.
- [S12] Besteiro, L. V.; Kong, X.-T.; Wang, Z.; Hartland, G.; Govorov, A. O. Understanding Hot-Electron Generation and Plasmon Relaxation in Metal Nanocrystals: Quantum and Classical Mechanisms. *ACS Photonics* **2017**, *4* (11), 2759–2781.
- [S13] Kong, X.-T.; Wang, Z.; Govorov, A. O. Plasmonic Nanostars with Hot Spots for Efficient Generation of Hot Electrons under Solar Illumination. *Adv. Opt. Mater.* **2017**, *5* (15), 1600594.